PCCP

RSC Publishing

PAPER

View Article Online
View Journal | View Issue

Nonergodicity in nanoscale electrodes

Diego Krapf*

Cite this: *Phys. Chem. Chem. Phys.*, 2013, **15**, 459

Received 14th August 2012,
Accepted 1st October 2012

DOI: 10.1039/c2cp42838e

www.rsc.org/pccp

The response of nanoscale electrodes displays deviations from conventional voltammetry theory that include a reduction in the limiting current and enhanced current fluctuations. We study the power spectra of these fluctuations in well characterized conical electrodes with radii between 2 and 10 nm. The fluctuations are found to display non-trivial power laws. We propose a model based on reversible adsorption of the redox species onto the nanoelectrode. This model is consistent with the non-stationary character of both the limiting current and the adsorption of molecules onto metal electrodes. Our model predicts the electrochemical reaction is nonergodic and sets fundamental limits on the sensitivity of uncoated nanoelectrodes.

1 Introduction

The exploration of fluidics at the nanoscale has shown an explosion in basic and applied sciences as well as in emerging technologies during the last decade. In particular, pores and channels of nanometer dimensions offer the possibility of studying biomolecules at their characteristic length scales. In order to fully exploit these systems their dimensions are reduced to the few-nanometer regime. A different kind of nanoscale fluid devices that has also given rise to several technological applications is based on electrochemical techniques. The unique size-dependent properties of nanostructured materials are employed to probe fundamental properties and to boost the applicability of preexisting technologies. These systems are finding their way in a great variety of applications such as solar cells,[1] high sensitive chemical- and bio-sensors[2–4] and in the study of heterogeneous kinetics and mass transport.[5] In addition, a nanometer-sized electrode, or nanoelectrode, can be used to study the electrochemical behavior of single molecules.[6–9]

Several challenges arise in the interpretation of nanoelectrode-based electrochemical data and deviations between experimental voltammetry and idealized mean field models are observed.[5,10–13] Different reasons have been proposed that would affect electrochemical currents in nanoelectrodes. These include transport within diffusion layers that have thicknesses of the same order of magnitude of the double layer and the structure of the double layer itself. Also, for such thin diffusion layers, the mean field assumption can lead to errors that may be avoided when Brownian dynamics are employed.[14,15] The magnitude of the deviations from conventional voltammetry theory remains controversial and it is probably a function of both the electrode material and the electroactive species. We have previously shown that the oxidation of $FcTMA^+$ at a gold nanoelectrode displays anomalous kinetics.[5] In particular, we found that the limiting current has a sublinear dependence on the concentration of electroactive ions, but the physical mechanism responsible for this anomaly is still unknown. Using $Ru(NH_3)_6^{3+}$ as electroactive species and Pt electrodes, Agyekum *et al.* have also shown that there are significant differences between the effective and the geometric radii when the electrode radius is smaller than 20 nm.[16]

In this report we address the problem of the deviations from classical electrochemistry in gold electrodes smaller than 10 nm by studying the current fluctuations. A nanoelectrode is immersed in a biased solution so as to drive an electrochemical reaction of an electroactive species (Fig. 1). The electrical current through the nanoelectrode provides a direct measure of the flux of electroactive species across the double layer. When high ionic strength solutions are used, the electric field is localized in the immediate vicinity of the nanoelectrode. Furthermore, because the concentration gradient is localized within a length scale comparable to the dimensions of the nanoelectrode, steep concentration gradients are achieved and transport properties are probed on the scale of several nanometers. We report on recorded enhanced fluctuations in the faradaic currents. These fluctuations are analyzed in terms of their power spectra and we find that the currents are non-stationary. The power spectra display non-trivial power laws which suggest weak ergodicity breaking in the electrochemical reaction. Not only these findings have direct implications of anomalous kinetics at the nanoscale, but they also place fundamental limitations on the signal-to-noise ratio attainable by nanoelectrode systems.

Electrical and Computer Engineering and School of Biomedical Engineering, Colorado State University, Fort Collins, CO 80523, USA.
E-mail: krapf@engr.colostate.edu; Tel: +1 970-491-4255

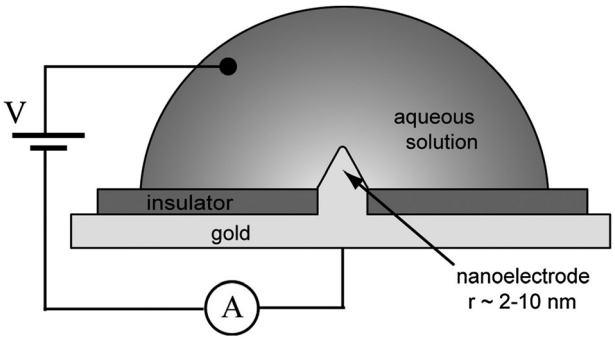

Fig. 1 Schematic representation of the electrochemical setup. A conical nanoelectrode is biased against a solution containing an electroactive ionic species and the current is recorded.

A process that displays ergodicity breaking has the interesting property that time and ensemble averages do not converge to the same values. These systems can exhibit aging properties related to their non-stationary behavior. At the core of many of the systems with broken ergodicity is a power law survival time distribution lacking a finite mean. As such, the behavior of these systems diverges from classical statistical physics and broadly accepted ideas, such as the fluctuation-dissipation theorem, need to be revisited.[17] We propose that in nanoelectrodes, ergodicity is broken by the reversible adsorption of the redox species onto the metal electrode.

2 Experimental section

Nanoelectrodes were fabricated by drilling a small pore in a thin insulating silicon nitride membrane and filling the pore with gold. Details of the fabrication process are described in ref. 18. Electrochemical measurements were recorded using a polydimethylsiloxane (PDMS) fluidic cell. A small opening in the fluid cell with a diameter of 150 μm contacts the nanoelectrode. A Ag/AgCl commercial electrode serving both as reference and counter electrode was placed at the other end of the cell. The current was recorded with a home-built amplifier having a gain of 10^{11} V A^{-1} and a bandwidth of 3 Hz. Current detection was carried out using an instrumentation op amp, selected for its low input voltage noise, in the inverting configuration with a 100 GΩ feedback resistor. The bandwidth of the circuit was limited by this feedback resistor in parallel with the parasitic capacitance of the connections. After current–voltage conversion, the signal was amplified another 100 times. The measurement system was set on a vibration isolation bench and the whole setup was enclosed inside a 3 mm-thick iron Faraday cage.

Ferrocenylmethyltrimethylammonium, $FcTMA^+$, was employed as the electroactive species and NH_4NO_3 (ammonium nitrate, Merck, Germany) was used as inert base electrolyte. FcTMA PF_6 was synthesized by metathesis of the iodide salt with NH_4PF_6.[19] Aqueous solutions were prepared with 18 MΩ cm water from a Milli-Q purification system (Millipore, Billerica, MA). In addition to the $FcTMA^+$ salt, 0.5 M excess base electrolyte was added to all solutions in order to obtain a constant ionic strength throughout all experiments. Prior to their use, solutions were microfiltered with 0.02 μm membranes (Whatman syringe filters, GE Healthcare).

3 Results

Cyclic voltammograms like the one shown in the inset of Fig. 2a have a sigmoidal shape characteristic of the steady-state response of micro- and nanoelectrodes. Repeated cyclic voltammetry between 200 and 600 mV shows the nanoelectrodes are stable over 36 h of continuous measurements.[18] Charge kinetics may influence the faradaic currents at potentials close to the half-wave. However, as the voltage is increased, the current becomes limited by the flow of reactants toward the electrode, which in principle is independent of applied voltage. A transport-limited plateau is observed at potentials higher than 0.5 V. At these potentials an enhancement of the fluctuations accompanies the faradaic currents. The fluctuations can be compared with the noise of the system by setting the potential at 580 mV and 300 mV, respectively. At the low voltage no faradaic currents are present and therefore, at this potential the noise is unrelated to the flow of electroactive species. A typical time-resolved curve, showing the recorded current at these two potentials, is shown in Fig. 2a. The dielectric response of the SiN insulating membrane that surrounds the nanoelectrode causes the observed initial decay.[18] A baseline (red line in the figure) is subtracted to the measurement to obtain the current fluctuations $\Delta i_n = i(t_n) - \overline{i(t)}$, where the time averaged $\overline{i(t)}$ denotes the baseline current. $\overline{i(t)}$ was empirically obtained by fitting the data to a three-component exponential function. The fluctuations were then analyzed both by means of their histogram and the power spectra $S_i(f)$.

We further examined the contribution of the voltage noise from the current–voltage (I–V) converter. This noise source has an amplitude that is proportional to dI/dV. At both analyzed potentials, 300 and 580 mV, $dI/dV \approx 0$ because in these situations, the reaction is far from the formal potential. In order to verify that the I–V converter does not have a significant contribution to the observed fluctuations, we measured the current near the half-wave potential where dI/dV is maximal (see inset of Fig. 2a). If the noise generated by the I–V converter significantly contributed to the background noise, the fluctuations near the formal potential would increase. Fig. 2b shows the current fluctuations at three potentials: 300, 440, and 580 mV. The data show that even though dI/dV at 440 mV is much greater than at 580 mV, the fluctuations are smaller. At this intermediate voltage, fluctuations of electrode potential may also play a role in the fluctuations of the faradaic current. In particular, the discreteness and stochastic nature of electron transfer events can cause the electrode potential to become a fluctuating variable.[39]

Histograms of the fluctuations from the mean current for a 5 nm nanoelectrode with 0.5 mM $FcTMA^+$ are shown in Fig. 3. For comparison, we also show the fluctuations from the mean when no electrochemical currents are present (V = 300 mV). For example, the standard deviation from the mean current for currents averaged over 1 s is found to be 11 fA, while the standard deviation of the external noise is only 0.8 fA.

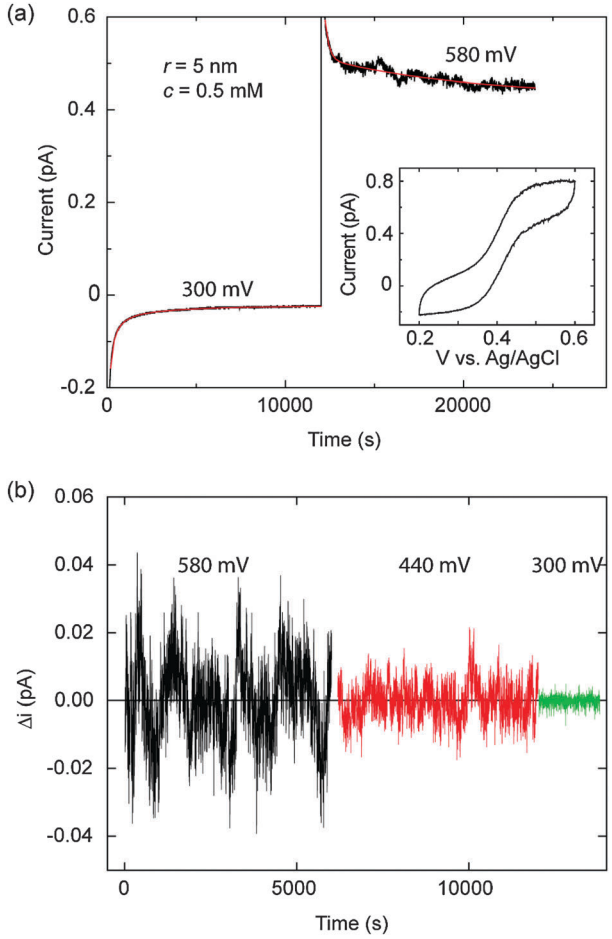

Fig. 2 Time resolved current probed at different potentials. (a) Data obtained with an electrode 5 nm in radius and $FcTMA^+$ concentration of 0.5 mM. The electrode was biased at 300 mV and 580 mV against the aqueous solution. The solid lines are third order exponentials that were fitted to the data in order to extract the mean current. The inset shows cyclic voltammogram measured under the same conditions. The observed hysteretic offset is caused by the parasitic dielectric response of the insulating SiN membrane that surrounds the electrode.[18] (b) Current fluctuations at three different potentials: 580, 440, and 300 mV. The fluctuations were obtained by subtracting the mean baseline from the raw data.

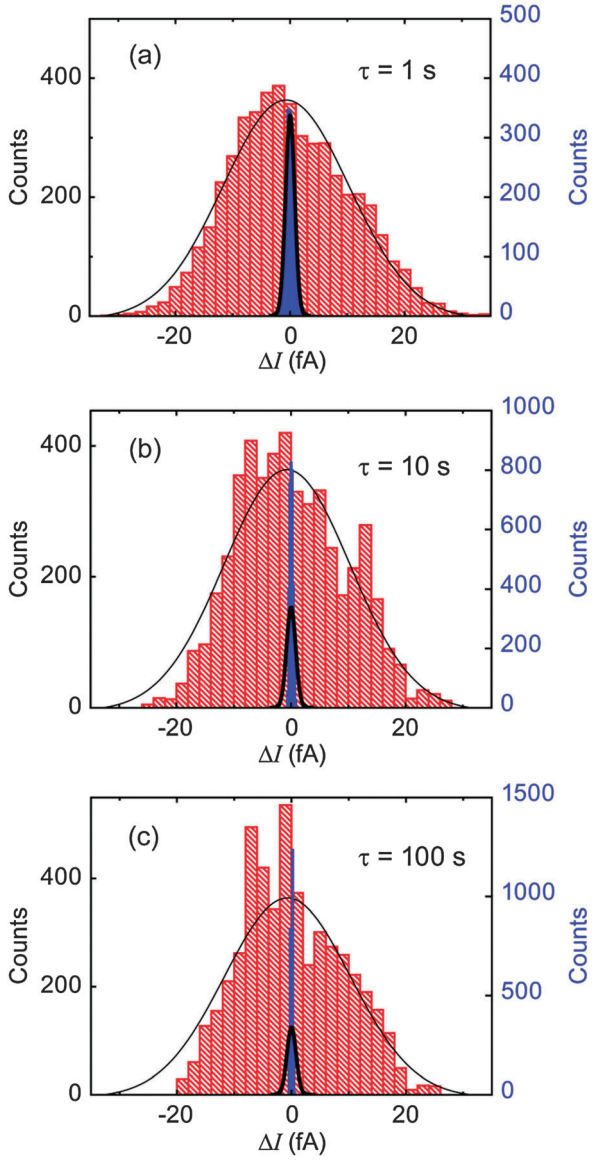

Fig. 3 Histograms of the fluctuations from the mean current. Each count represents a current measurement averaged over a time interval. Data were taken with a 5 nm electrode at a $FcTMA^+$ concentration of 0.5 mM. Also shown (narrower distributions, right *Y* axis) are the histograms of the fluctuations when the potential is set at 300 mV and thus, no faradaic current is recorded. The bin size is 2 fA for the faradaic current fluctuations and 0.2 fA for the fluctuations at 300 mV. (a) Current is averaged over 1 s. (b) Current averaged over 10 s. (c) Current averaged over 100 s. The lines represent fittings to Gaussian probability distributions of the histograms averaged over 1 s. The same lines are plotted for comparison in the histograms averaged over longer times.

Therefore, at this concentration, the noise is governed by the electroactive ion flow. Based on the central limit theorem, one expects that averaging over longer measurement times would reveal narrower distributions. Surprisingly, the width of faradaic current fluctuations distribution is not affected by the duration of the averaging time window (Fig. 3b and c). Increasing the averaging time appears to clip the tails of the distribution but the overall width of the distribution does not change. On the other hand, the distribution of the external noise sharply narrows when the averaging time window increases from 1 s (Fig. 3a) to 10 s (Fig. 3b) to 100 s (Fig. 3c).

Fig. 4 shows the power spectra of the fluctuations in the electrochemical current. In Fig. 4a we show spectra related to different redox couple concentrations (c = 0, 0.03, 0.3 and 0.5 mM) with a 5 nm nanoelectrode. All the spectra display a non-trivial $1/f^{\beta}$ behavior with an exponent $\beta = 1.27 \pm 0.05$. The power spectrum of the 0.5 mM concentration shows $1/f^{\beta}$ noise spanning three decades, *i.e.*, the whole probed frequency range, from 1 mHz to 1 Hz. When the concentration decreases, the spectral density exhibits two distinctive distribution functions in different frequency windows. $1/f^{\beta}$ noise appears below a critical frequency and white noise dominates the spectrum above it. Both the $1/f^{\beta}$ and the frequency-independent components scale with the ion concentration. However, in all the measurements, the intensity of the frequency-independent part

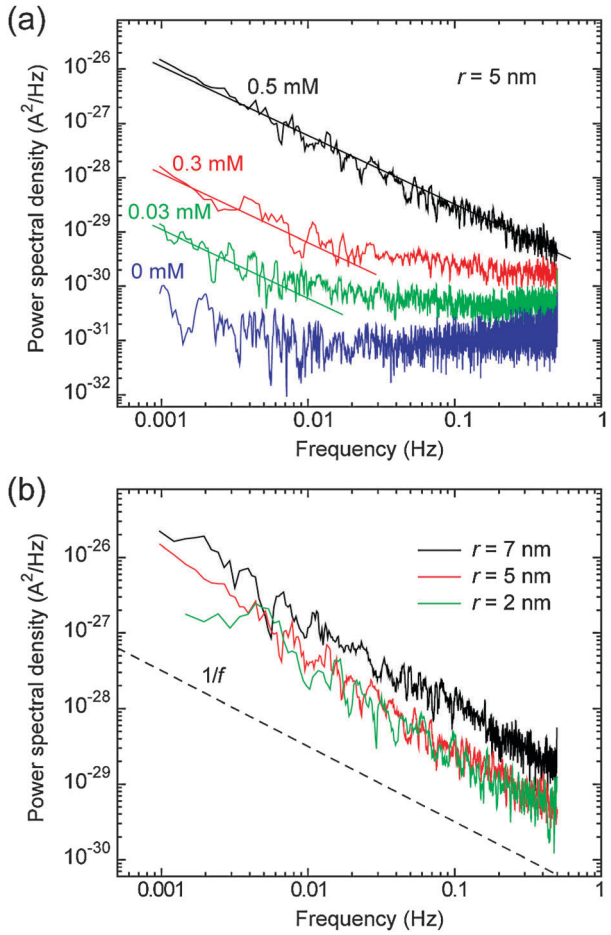

Fig. 4 Power spectral density $S_I(f)$ of the current fluctuations. (a) Spectra obtained for 4 different concentrations (c = 0, 0.03, 0.3, and 0.5 mM) at an electrode 5 nm in radius. The spectrum of the zero concentration indicates the response of the system when no electroactive species is present. The three solid lines indicate $1/f^{\beta}$ with $\beta = 1.27$. (b) Spectra of three different nanoelectrodes with radii of 2, 5, and 7 nm. A $1/f$ plot is shown for comparison.

of the spectrum is much higher than shot-noise. For example, at 0.5 mM, $S_{shot}(f) = 2eI = 1.5 \times 10^{-31}$ A^2 Hz^{-1}, while $S(f) > 3 \times 10^{-30}$ A^2 Hz^{-1}, for the whole frequency range. At zero concentration, the noise is mainly white and its intensity is $\sim 10^{-31}$ A^2 Hz^{-1}, which characterizes the r.m.s. noise of our experimental setup (0.3 fA Hz$^{-1/2}$). In Fig. 4b the power spectra of electrodes with radii of 2, 5, and 7 nm are shown for a concentration of 0.5 mM. Again, a $1/f^{\beta}$ behavior with a similar exponent is observed with the different electrodes.

4 Discussion

In electrochemical systems, an ion in solution can transiently bind to the electrode. This process takes place on very different time scales from electron transfer kinetics. The latter is a fast reaction, that depends exponentially on the applied potential, $K_{el} \sim \exp[e(V - V_0)/k_BT]$, where V is the applied potential, V_0 the formal potential of the reaction (V_0 = 0.42 V), e the electron charge, and k_BT the thermal energy.[20] Thus, at the potential of our experiments, $e(V - V_0)/k_BT = 6.4$. However, after oxidation, $FcTMA^{2+}$ molecules can remain bound to the nanoelectrode during a much longer time. Because both the reactant ($FcTMA^{+}$) and the product ($FcTMA^{2+}$) are positively charged, a bound ion would affect the flux of reactants to the electron surface *via* electrostatic interactions. However, mass transport is only impacted by reversible adsorption when the size of the electrode is comparable to the Debye length. In the surrounding of a nanoscale electrode, the flux inhibition is enhanced by the characteristic steep concentration profiles.[5]

We propose that oxidized $FcTMA^{2+}$ molecules reversibly adsorb onto the nanoelectrode. A dissociation rate constant K_{off} introduces a survival probability, *i.e.*, the probability that a molecule is still bound to the nanoelectrode after time t, of the form $P_S(t) = e^{-K_{off}t}$. Thus, the probability density function of bound times is $\psi(t) = K_{off}e^{-K_{off}t}$. However, if we consider a certain degree of heterogeneity in the surface of the electrode, a hierarchy of binding sites may arise. In this case, anomalous kinetics develops when the system is out of equilibrium, a condition that is maintained in the biased nanoelectrode.[5]

The adsorption of ions at electrochemical interfaces has very complex dynamics that are not fully understood.[21] Lemay *et al.* have recently shown that the dynamic adsorption of different ferrocene derivatives onto metal electrodes is dependent on both the applied potential and the history of the device.[22,23] Interestingly, it was observed that the amount of adsorption varied slowly over time.[23] These data provide strong evidence for the adsorption of redox species onto metal electrodes with a distribution of trapping energies. The fact that adsorption is extremely sensitive to trace contaminants also leads to a broadening of the trapping energy distribution.

A similar problem that was modelled by Saxton[24,25] is a hierarchy of traps that affects the diffusion of molecules in the cytoplasm and plasma membrane of live cells. If molecules are continually trapped by potential wells whose depths are exponentially distributed, the distribution of binding times follows a power-law,

$$\psi(t) \sim t^{-(1+\alpha)}. \quad (1)$$

A particularly interesting situation arises when $0 < \alpha < 1$, because the mean binding time diverges. Under these conditions, the system displays aging and nonergodicity.[17,26] Such Lévy statistics were experimentally observed in different systems, including quantum dot blinking,[27–29] gating fluctuations in ion channels,[30] and diffusion on the surface of mammalian cells[31] and in the yeast cytoplasm.[32] Eqn (1) is analogous to a power law in the dissociation rate constants with $P(K) \sim K^{-(1-\alpha)}$, for small K, which derives from an exponential distribution in binding energies, $P(E_B) \sim \exp(-\alpha E_B/k_BT)$. So, even though the binding time distribution is very broad, the distribution of binding energies is narrow in the sense that all moments are finite.

Multiple ions could simultaneously adsorb reversibly onto the nanoelectrode. As each new ion is adsorbed, the flux of electroactive species toward the electrode is further inhibited. This inhibition, in

turn, reduces the faradaic current. The reaction has then a large number of possible states,

$$S_0 \underset{k^-}{\overset{k^+}{\rightleftharpoons}} S_1 \underset{k^-}{\overset{k^+}{\rightleftharpoons}} S_2 \underset{k^-}{\overset{k^+}{\rightleftharpoons}} \dots \underset{k^-}{\overset{k^+}{\rightleftharpoons}} S_m \underset{k^-}{\overset{k^+}{\rightleftharpoons}} \dots \quad (2)$$

where m is the number of ions bound to the electrode at a given time, k^+ is the rate of binding of a new ion to the metal and is related to the total reactant flux j and to the concentration by a factor $\eta < 1$, $k^+ = \eta c$. We assume the dissociation rate k^- is such that it yields eqn (1). Rigorously, $k^{+/-}$ depend on the number of ions m, with k^+ decreasing with m and k^- expected to increase with m.

To simplify the modelling and reduce the number of unknowns, we model the system in a binary fashion. In other words, two states are considered: a free state S_0 (as in eqn (2)), and a bound state S_1 at which the electrochemical current is lower due to the inhibition of ion flux,

$$S_0 \underset{k^-}{\overset{k^+}{\rightleftharpoons}} S_1. \quad (3)$$

This system behaves similar to other nonergodic binary systems, such as quantum dots, that were extensively studied.[33,34]

Given the nature of electrochemical measurements, the time distribution of binding times is not readily accessible from experimental data. On the other hand, the fluctuations can be directly probed in the frequency domain. The power spectrum for a two-state process obeying Lévy statistics has been analyzed.[35,36] Processes following eqn (1) display a power spectrum with $1/f^{\beta}$ behaviour, where $\beta = 2 - \alpha$. The data presented in Fig. 4 indicate that the residence time in state S_1 follows a binding time distribution according to eqn (1) with $\alpha = 0.73 \pm 0.05$.

A power law behaviour with $0 < \alpha < 1$ has striking consequences. The absence of a finite mean binding time, *i.e.*, $\int_0^{\infty} t\psi(t)\mathrm{d}t = \infty$, implies that the temporal average of a time series is a random variable that does not converge to the ensemble mean. If the process were Markovian, as $t \to \infty$ the time average would converge to a deterministic value with zero variance. However, in the nonergodic situation the time average is a random variable. In simpler terms, the measured currents are irreproducible values. An example of how the electrochemical measurements are stochastic can be seen in Fig. 5a. Here the voltage is stepped back and forth between 300 and 580 mV in 60 min intervals. Each step in voltage produces a different result between 0.83 pA and 1.0 pA. The hypothesis of ergodicity breaking also implies that the power spectrum for a given measurement time and fixed physical conditions would become a random variable. In Fig. 5b, we see the random nature of the power spectra, consistent with the random nature of the currents.

The picture where the time average is a random variable itself is consistent with observations that the dynamics of adsorption vary over time.[23] This change of the absorption over time is an aging process that can be rigorously derived from a binding time power law distribution (eqn (1)) and it implies that for a given time series the time averaged faradaic current decreases with experimental time. In our model, when an ion

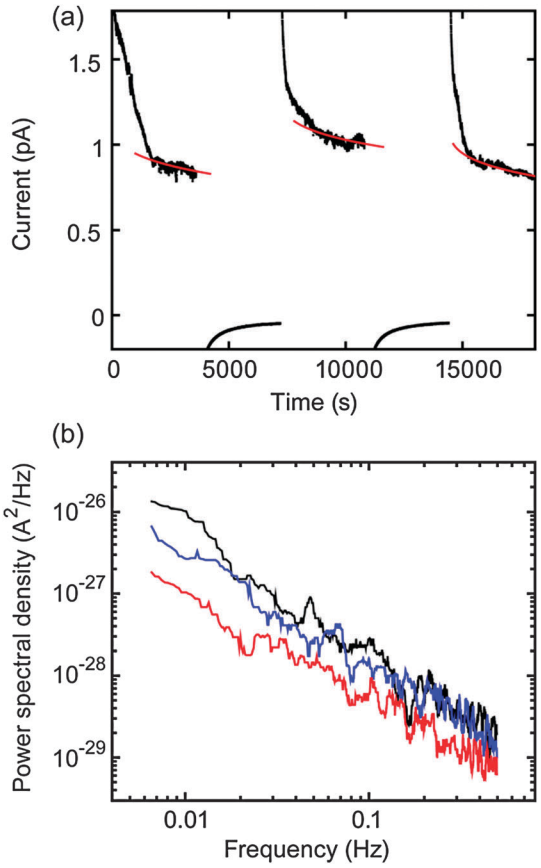

Fig. 5 Electrochemical response of a 7 nm electrode. (a) Time series of the current obtained by alternating the voltage between 300 mV and 580 mV every 3600 s. Note how the current in the second series at 580 mV is higher than the first one, while that in the third series is lower. Again, strong fluctuations at the oxidation potential are seen while no fluctuations are evident at 300 mV. Aging behavior is observed and it is modeled by eqn (8) in the main text. The three red lines show power laws $I = I_0 - Bt^{1-\alpha}$ with $\alpha = 0.73$. The initial decay is due to the SiN membrane dielectric response. (b) Power spectra of the fluctuations in the time series at 580 mV. The amplitude of the spectra appears be a random variable with a striking scatter from one spectrum to another.

binds to the nanoelectrode, the state S_1 becomes occupied and the current is inhibited. In probability terms, if $P_1(t)$ is the probability that S_1 is occupied at time t, the nanoelectrode senses an effective change in ionic concentration $\delta_c = -\lambda P_1(t)$. Thus,

$$I(t) = \gamma[c - \lambda P_1(1)]. \quad (4)$$

where γ is a proportionality factor that depends on electrode size and shape.[6] From eqn (3), at any given time $P_1(t) = (k^+/k^-)P_0$ and we can find the time dependence of k^- from scaling arguments.[37] In a stationary system, $k^- = 1/\langle\tau\rangle$, where $\langle\tau\rangle$ is the mean binding time. In our non-stationary model, $\langle\tau\rangle$ depends on the experimental time t,

$$\langle\tau\rangle = \int_0^t \tau\psi(\tau)\mathrm{d}\tau. \quad (5)$$

Given that $\psi(\tau) \sim t^{-(1+\alpha)}$, the mean binding time scales as

$$\langle\tau\rangle \sim t^{1-\alpha}. \quad (6)$$

Then we can rewrite eqn (4) as

$$I(t) = \gamma(c - \lambda_1 k^+ P_0 t^{1-\alpha}). \quad (7)$$

Fort "short" times, $P_1 \ll P_0$, we can assume P_0 is a constant and k^+ is proportional to c. Thus, the faradaic current has a term that decays as $-t^{1-\alpha}$,

$$I(t) = \gamma c(1 - \lambda_2 t^{1-\alpha}). \quad (8)$$

Fig. 5 shows this aging behavior in the three curves at 580 mV. Each time series is fit to eqn (8) using $\alpha = 0.73$.

For longer times than those supported by eqn (8), in our two-state system, $P_0 + P_1 = 1$. Therefore

$$P_1 = k^+/(k^+ + k^-), \quad (9)$$

and we see that the condition $P_1 \ll P_0$ holds when $At^{\alpha-1} \gg k^+$ (A is a constant of proportionality between $t^{\alpha-1}$ and k^-). Using the same scaling arguments and combining eqn (4) and (9), we obtain

$$I(t) = \gamma\left[c - \frac{\lambda}{1 + (A/k^+)t^{\alpha-1}}\right]. \quad (10)$$

For blinking quantum dots, the $1/f$ power spectrum depends on the measurement time T. In a similar way, we expect the aging properties of adsorption onto metallic nanoelectrodes to be observed in the power spectrum for different measurement times. Fig. 6a shows the power spectra of a nanoelectrode computed over 512, 1024, 2048, 4096, and 8192 points in the faradaic current fluctuations time series. As the total experimental time increases a minor decrease in the amplitude of the power is seen. Margolin and Barkai calculated the dependence of the power spectrum of a two-state process obeying Lévy statistics on the experimental time T.[35] It was found that the power spectrum scales as $T^{-(1-\alpha)}$. Our experimental data indicates $1 - \alpha = 0.27$. Even though the changes in the spectra are barely above the noise levels, it is interesting to see in Fig. 6b that when the power spectra are factored by $T^{0.27}$ the apparent scaling of the spectra shrinks.

The kinetics of the reaction are expected to be anomalous with non-linearities as those observed in ref. 5. This is not obvious from eqn (8) and (10), but non-linearities arise from the fact that the on/off-rates depend on the concentrations. At higher concentrations, k^+ increases and, thus, the lack of the mean of the dissociation time has a greater impact on the faradaic current. A closer look at eqn (6) and (8) reveals that the prefactor in eqn (6) depends on the concentration because the faster the system explores more binding sites, it will converge to eqn (6) in a more rapid way. Thus, λ_2 depends on c. These anomalous kinetics are analogous to nonergodic subdiffusion processes modelled by a continuous time random walk with power-law stalling time distributions.[38]

How valid are the estimates from the power spectra if each measurement yields a different current? Niemann *et al.* showed that even though the time averages are random variables, the fluctuations only affect the prefactor for the whole power spectrum and the measurement of the exponent β in the $1/f^\beta$ behavior is not hindered by weak ergodicity breaking.[36] The extent of the variance of the time averages will depend on the actual binding rate k^+. Furthermore, for very long times not accessed in our measurements a cutoff in the binding time distribution exists, leading to a current saturation described by eqn (10). For example, the on and off periods of CdSe nanocrystals exhibit a cutoff of several tens of seconds after which the sojourn time distributions decay more rapidly.[28] Given the results presented here, in Au nanoelectrodes the cutoff appears to be longer than a few hours.

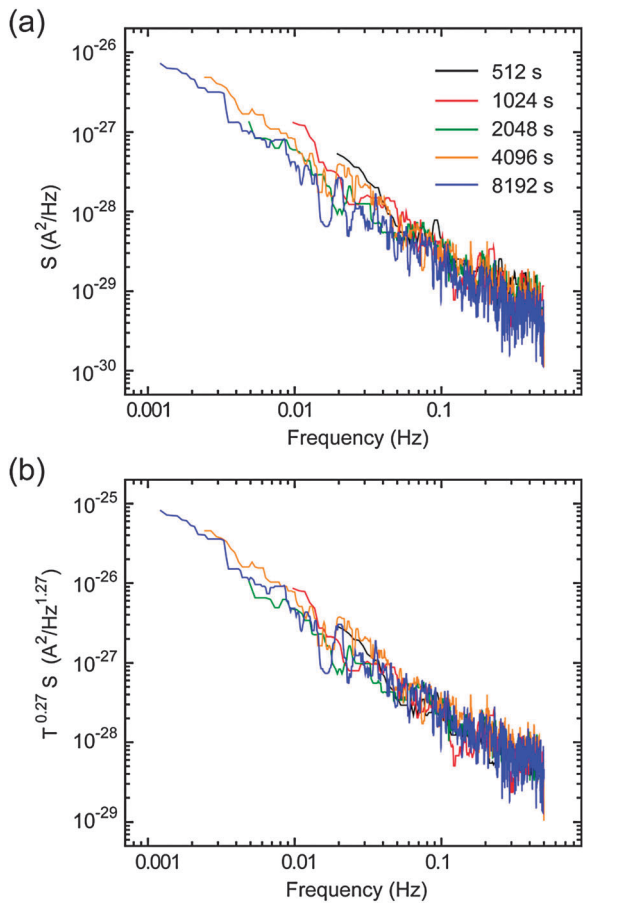

Fig. 6 Power spectral density calculated from time series measured over different experimental times. (a) Five power spectra calculated from a single measurement that was truncated at different times: 512 s, 1024 s, 2048 s, 4096 s, and 8192 s. (b) Each power spectra in (a) was scaled by $T^{1-\alpha}$, where T is the experimental time and $\alpha = 0.73$.

5 Conclusions

We measured $1/f^\beta$ noise in the conductivity of aqueous solution when the $FcTMA^+$ transport is localized within nanometers of a Au electrode. Ion transport was probed with nanoelectrodes stable over periods longer than 36 hours, allowing us to investigate the

low frequency regimes. We propose that the observed noise is a consequence of reversible adsorption of the reactive species onto the metal nanoelectrode. Our measurements are consistent with a model where there is a broad distribution of binding times, which introduces long-time correlations and ergodicity breaking in the faradaic current. This model explains the power-law fluctuations in the faradaic current, the non-stationary behavior in nanoelectrodes, and the non-linearities observed in mass transport at the nanoscale.[5] These anomalies in mass transport set fundamental limiting factors in nanofluidic applications.

Acknowledgements

I acknowledge the support of the National Science Foundation through grant 0956714. This work was partially done at the Kavli Institute of Nanoscience, Delft University of Technology. I want to thank Serge Lemay for helping with the experimental design, useful discussions and reading the manuscript.

Notes and references

1 D. A. Rider, R. T. Tucker, B. J. Worfolk, K. M. Krause, A. Lalany, M. J. Brett, J. M. Buriak and K. D. Harris, *Nanotechnology*, 2011, **22**, 085706.
2 X. J. Zhang, J. Wang, B. Ogorevc and U. E. Spichiger, *Electroanalysis*, 1999, **11**, 945.
3 J. J. Fei, K. B. Wu, F. Wang and S. S. Hu, *Talanta*, 2005, **65**, 918.
4 W. Z. Wu, W. H. Huang, W. Wang, Z. L. Wang, J. K. Cheng, T. Xu, R. Y. Zhang, Y. Chen and J. Liut, *J. Am. Chem. Soc.*, 2005, **127**, 8914.
5 D. Krapf, B. M. Quinn, M. Y. Wu, H. W. Zandbergen, C. Dekker and S. G. Lemay, *Nano Lett.*, 2006, **6**, 2531.
6 F. R. F. Fan and A. J. Bard, *Science*, 1995, **267**, 871.
7 M. W. Holman, R. C. Liu and D. M. Adams, *J. Am. Chem. Soc.*, 2003, **125**, 12649.
8 C. Amatore, F. Grun and E. Maisonhaute, *Angew. Chem., Int. Ed.*, 2003, **42**, 4944.
9 F. J. M. Hoeben, F. S. Meijer, C. Dekker, S. P. J. Albracht, H. A. Heering and S. G. Lemay, *ACS Nano*, 2008, **2**, 2497.
10 W. S. Baker and R. M. Crooks, *J. Phys. Chem. B*, 1998, **102**, 10041.
11 R. B. Morris, D. J. Franta and H. S. White, *J. Phys. Chem.*, 1987, **91**, 3559.
12 Y. Sun, Y. W. Liu, Z. X. Liang, L. Xiong, A. L. Wang and S. L. Chen, *J. Phys. Chem. C*, 2009, **113**, 9878.
13 J. Lakbub, I. Kady and P. Sun, *Electroanalysis*, 2011, **23**, 2205.
14 B. Corry, S. Kuyucak and S. H. Chung, *Biophys. J.*, 2000, **78**, 2364.
15 S. Edwards, B. Corry, S. Kuyucak and S. H. Chung, *Biophys. J.*, 2002, **83**, 1348.
16 I. Agyekum, C. Nimley, C. X. Yang and P. Sun, *J. Phys. Chem. C*, 2010, **114**, 14970.
17 S. Burov, R. Metzler and E. Barkai, *Proc. Natl. Acad. Sci. U. S. A.*, 2010, **107**, 13228.
18 D. Krapf, M. Y. Wu, R. M. M. Smeets, H. W. Zandbergen, C. Dekker and S. G. Lemay, *Nano Lett.*, 2006, **6**, 105.
19 S. G. Lemay, D. M. van den Broek, A. J. Storm, D. Krapf, R. M. M. Smeets, H. A. Heering and C. Dekker, *Anal. Chem.*, 2005, **77**, 1911.
20 A. J. Bard and L. R. Faulkner, *Electrochemical Methods: Fundamentals and Applications*, Wiley, New York, NY, 2001.
21 O. M. Magnussen, *Chem. Rev.*, 2002, **102**, 679.
22 P. S. Singh, H. S. M. Chan, S. Kang and S. G. Lemay, *J. Am. Chem. Soc.*, 2011, **133**, 18289.
23 S. Kang, K. Mathwig and S. G. Lemay, *Lab Chip*, 2012, **12**, 1262.
24 M. J. Saxton, *Biophys. J.*, 2007, **92**, 1178.
25 M. J. Saxton, *Biophys. J.*, 2008, **94**, 760.
26 E. Barkai, *Phys. Rev. Lett.*, 2003, **90**, 104101.
27 K. T. Shimizu, R. G. Neuhauser, C. A. Leatherdale, S. A. Empedocles, W. K. Woo and M. G. Bawendi, *Phys. Rev. B: Condens. Matter Mater. Phys.*, 2001, **63**, 205316.
28 X. Brokmann, J. P. Hermier, G. Messin, P. Desbiolles, J. P. Bouchaud and M. Dahan, *Phys. Rev. Lett.*, 2003, **90**, 120601.
29 P. Frantsuzov, M. Kuno, B. Janko and R. A. Marcus, *Nat. Phys.*, 2008, **4**, 519.
30 W. Nadler and D. L. Stein, *Proc. Natl. Acad. Sci. U. S. A.*, 1991, **88**, 6750.
31 A. V. Weigel, B. Simon, M. M. Tamkun and D. Krapf, *Proc. Natl. Acad. Sci. U. S. A.*, 2011, **108**, 6438.
32 J. H. Jeon, V. Tejedor, S. Burov, E. Barkai, C. Selhuber-Unkel, K. Berg-Sorensen, L. Oddershede and R. Metzler, *Phys. Rev. Lett.*, 2011, **106**, 048103.
33 G. Margolin and E. Barkai, *Phys. Rev. Lett.*, 2005, **94**, 080601.
34 F. D. Stefani, J. P. Hoogenboom and E. Barkai, *Phys. Today*, 2009, **62**, 34–39.
35 G. Margolin and E. Barkai, *J. Stat. Phys.*, 2006, **122**, 137–167.
36 M. Niemann, I. G. Szendro and H. Kantz, *Chem. Phys.*, 2010, **375**, 370–377.
37 E. Barkai, Y. Garini and R. Metzler, *Phys. Today*, 2012, **65**, 29–35.
38 I. M. Sokolov, J. Klafter and A. Blumen, *Phys. Today*, 2002, **55**, 48–54.
39 V. García-Morales and K. Krischer, *Proc. Natl. Acad. Sci. U. S. A.*, 2010, **107**, 4528–4532.